Supporting Information for

Strong and Electrically Conductive Graphene Based Composite Fibers and Laminates

Ivan Vlassiouk,[1*] *Georgios Polizos,*[1] *Ryan Cooper,*[1] *Ilia Ivanov,*[1] *Jong Kahk Keum,*[1] *Felix Paulauskas,*[1] *Panos Datskos*[1] *and Sergei Smirnov*[2]

[1]Oak Ridge National Laboratory, Oak Ridge, TN, USA, 37830

[2]Department of Chemistry and Biochemistry, New Mexico State University, NM, USA, 88011

* Corresponding author email: vlassioukiv@ornl.gov

I. ***Optical/SEM characterization of fibers/scrolls.***

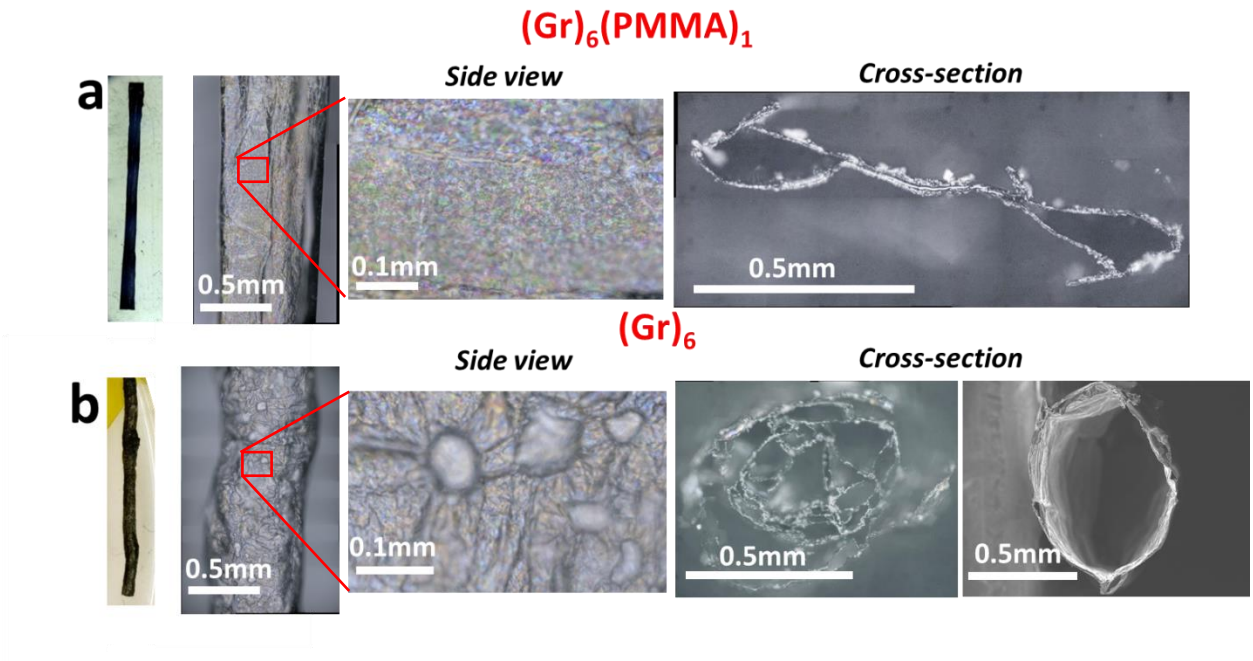

Figure S1. *Optical and SEM images of Type 2 samples – scrolls of 2'' wide sheets prepared on a 0.7 mm diameter wire.* **a.** Optical images of a $(Gr)_6(PMMA)_1$ scroll/fiber. A multilayered scroll is clearly seen on the cross-section image. **b.** Optical images of a $(Gr)_6$ scroll prepared by dissolving PMMA in acetone from the sample shown in (a). Acetone may remain trapped in the fiber structure even after annealing, as suggested by blisters visible on the side view, and contribute to the observed lowering of the strength and stiffness of pure graphene fibers described in the main text. Cross-section of this $(Gr)_6$ sample varied across the fiber length from purely scroll-type (SEM image on the right) to a more complex structure shown on the optical image of the cross-section. Estimated number of graphene layers ~140 (see main text).

II. Mechanical characterization of scrolls/fibers

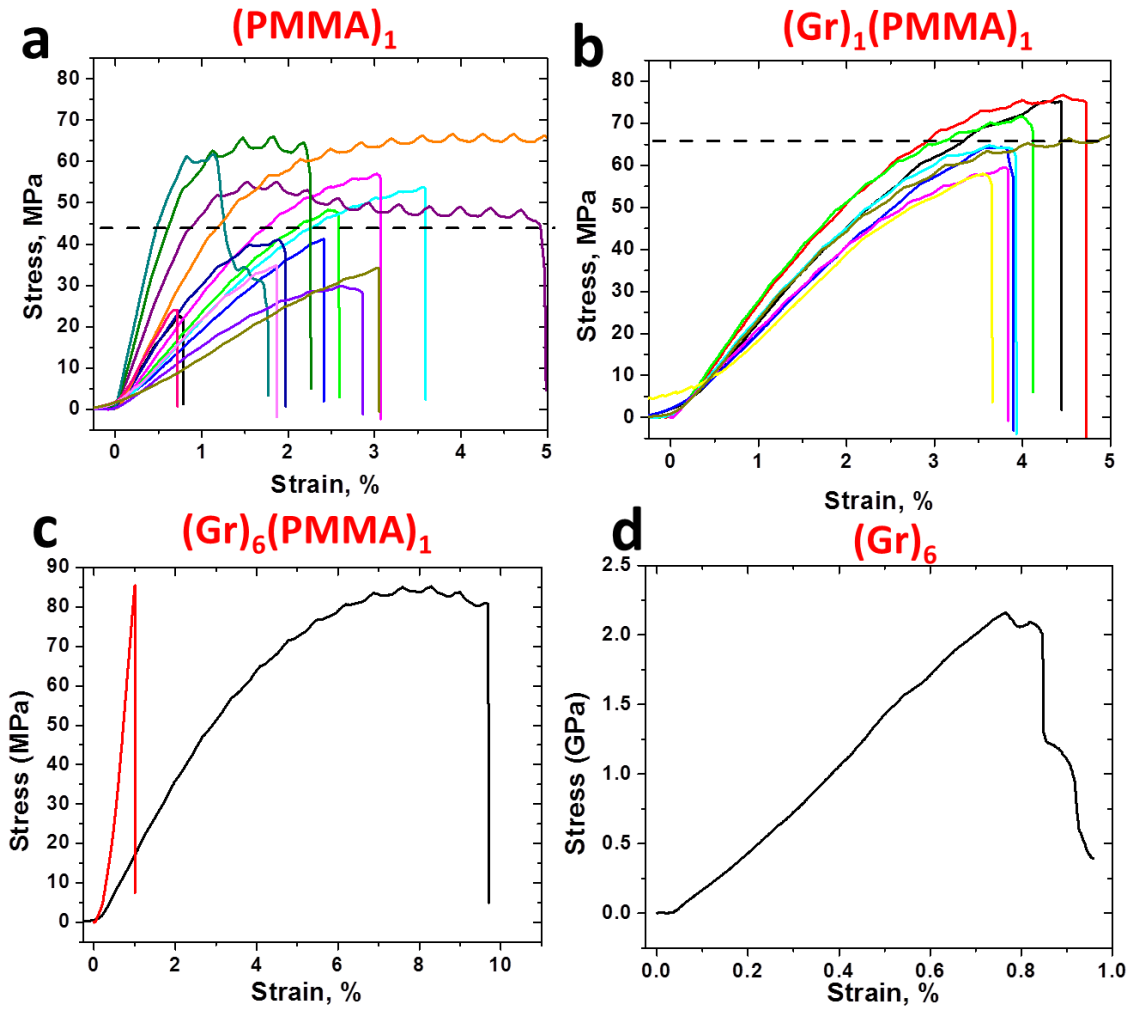

Figure S2. *Strain-Stress curves for Type 2 samples (scrolls/fibers).* **a.** Pure PMMA fibers $(PMMA)_1$ **b.** Single layer graphene with single layer PMMA fibers,–*i.e.*, $(Gr)_1(PMMA)_1$ fibers. **c**. Consequently transferred six layers of graphene on single PMMA layer, *i.e.*, $(Gr)_6(PMMA)_1$ fibers. **d.** Six layers graphene fiber $(Gr)_6$ prepared by PMMA dissolution from $(Gr)_6(PMMA)_1$ fiber overnight.

$(PMMA)_1$ scrolls showed large variation in both the strength and modulus (Figure S2a). Average measured strength was 43.5 ± 15.5 MPa (Figure S2a) whereas $(Gr)_1(PMMA)_1$ scrolls showed much less variability and the strength was equal to 68 ± 7.7 MPa (Figure S2b). Using the rule of mixtures with graphene's volume, $V_{Gr} = (1.3\pm0.2)\cdot10^{-3}$, we estimate the effective graphene strength to be 19±9 GPa for these samples. For $(Gr)_6(PMMA)_1$ scrolls and for $(Gr)_6$ scrolls obtained from the former by dissolving PMMA the measured strength are lower, 4 GPa and 2.2 GPa, correspondingly. $(Gr)_6(PMMA)_1$ scrolls also showed wider variability in the modulus, with

the best values up to 1.1 TPa (red curve, Figure S2c), while $(Gr)_6$ scrolls showed 0.3 TPa modulus.

Strain-Stress curves were measured on either homemade setup [1], or Linkam Instruments TST350 (Type 1 samples) or MTS Alliance RT/5 instrument (Type 2 samples).

III. Measurements of the thicknesses of prepared laminates.

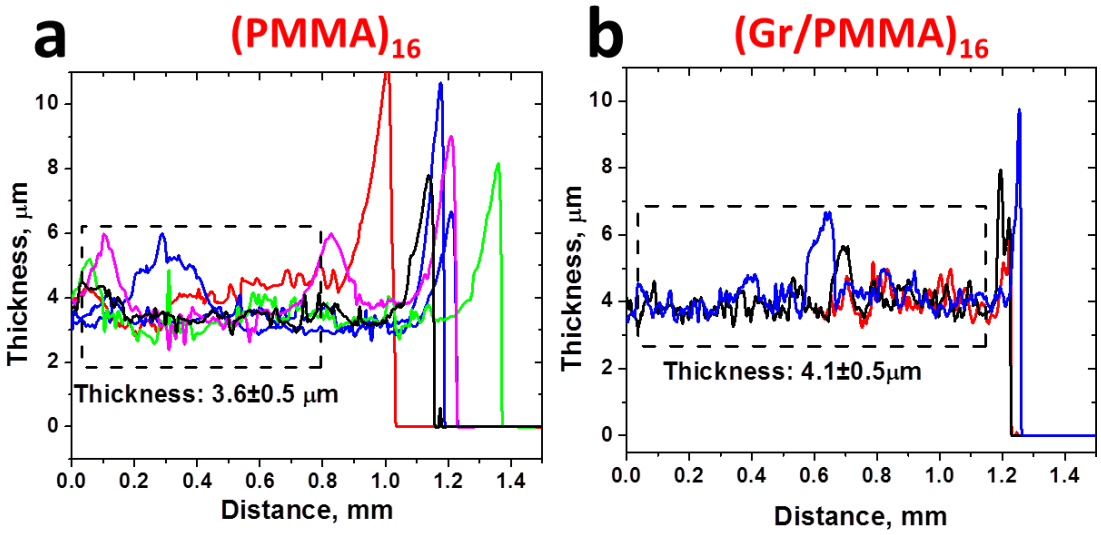

Figure S3. Thickness of the laminates was measured by a Dektak profilometer. Thickness of the $(PMMA)_{16}$ laminates was measured to be 3.6 ± 0.5μm (**a**) while $(Gr/PMMA)_{16}$ laminates had thickness of 4.1 ± 0.5 μm (**b**). Dashed squares show the regions of analyzed thickness. Applied stresses showed in Figure 2c of main text were calculated using these thicknesses.

IV. 2D Grazing-incidence wide-angle X-ray scattering (GIWAXS) for laminates.

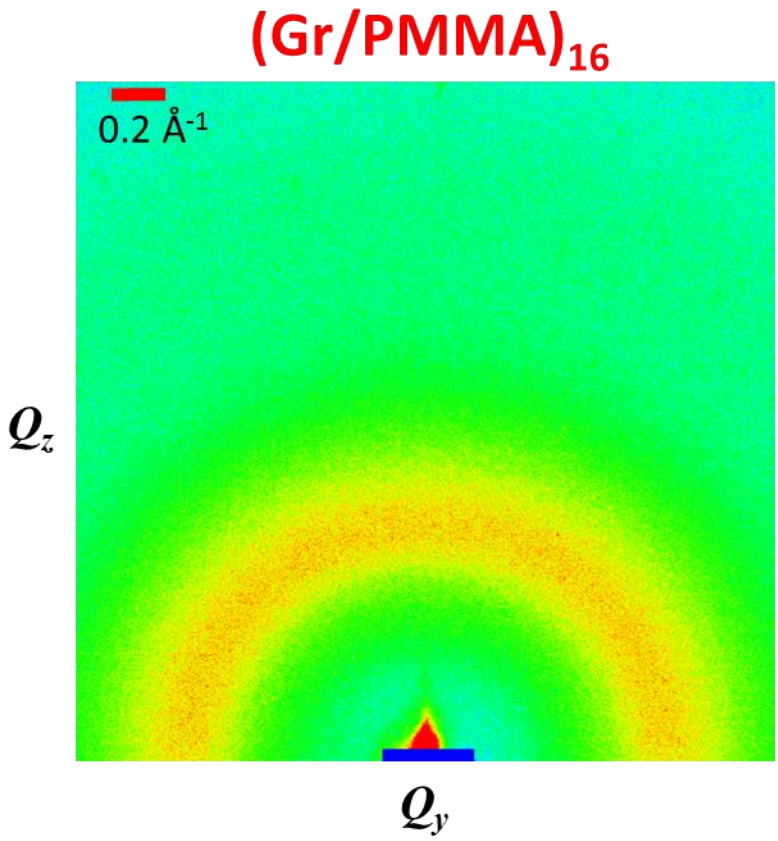

Figure S4. *2D Grazing-incidence wide-angle X-ray scattering (GIWAXS) pattern*. Obtained Grazing-incidence wide-angle X-ray scattering does not show any preferential orientation of the PMMA chain in $(Gr/PMMA)_{16}$ laminates.

GIWAXS measurements were carried out on an Anton Paar SAXSess mc^2 equipped with a multipurpose VarioStage. The diffracted beam was recorded on an imaging plate (Multisensitive Storage Phosphor) and read using a Perkin Elmer Cyclon 2D imaging plate reader. For the GIWAXS measurements, X-ray was generated at 40 kV/50 mA and X-ray beam wavelength was λ =1.541 Å (Cu Ka radiation) and the grazing incidence angle was 0.2^0. The global orientation of amorphous PMMA chains for different films can be probed using two-dimensional (2D) grazing-incidence wide-angle X-ray scattering (GIWAXS). Figure S4 shows the collected 2D GIWAXS patterns for $(Gr/PMMA)_{16}$ film. In order to conduct 2D GIWAXS measurements, a laminate was put on a 300 nm SiO_2/Si wafer. If PMMA chains were oriented along the in-plane direction due to confinement, the scattering would be concentrated around the out-of-plane direction by forming a narrow arc. However, the 2D GIWAXS pattern in Figure S4 merely exhibits isotropic halo indicating that the PMMA chains are in a randomly oriented state because R_g (~25nm)[5,6] is an order of magnitude smaller than the PMMA film thickness (250nm).

V. Differential Scanning Calorimetry of laminates.

Differential Scanning Calorimetry data were obtained on a TA Instruments Q2000 using ~1mg (~2cm^2) of laminates. Specimens were encapsulated in aluminum pans, and two heating scans were performed from room temperature to 180^{0}C with the temperature ramp 10^{0}C/min. All runs were performed in nitrogen. The glass transition temperature for $(Gr/PMMA)_{16}$ sample, T_g =122^{o}C, was 3 degrees lower than that for $(PMMA)_{16}$, T_g = 125^{o}C. Lowering of T_g in $(Gr/PMMA)_{16}$ indicates weaker interactions between PMMA and graphene as compared to PMMA-PMMA. [2,3,4] Prior to the DSC scans both samples were annealed in the measurement cell at 180 ^{o}C and thereafter were quenched to room temperature under the same cooling rate (10 ^{o}C/min) in order to erase their thermal history. The reported decrease in the Tg value was reproducible in both, heating and cooling scans.

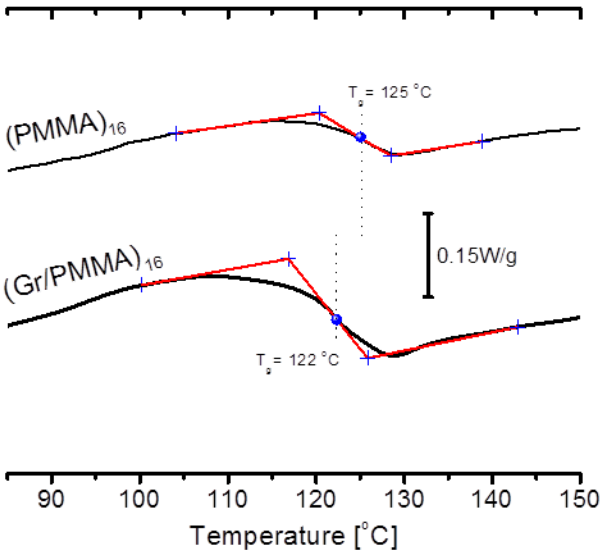

Figure S5. *Differential Scanning Calorimetry thermogram of the second heating scan for $(PMMA)_{16}$ and $(Gr/PMMA)_{16}$ samples.* The circles (•) indicate the glass transition temperature, which corresponds to the inflection point of the step change. For clarity, the curves are shifted vertically.

VI. Additional images of suspended LEDs

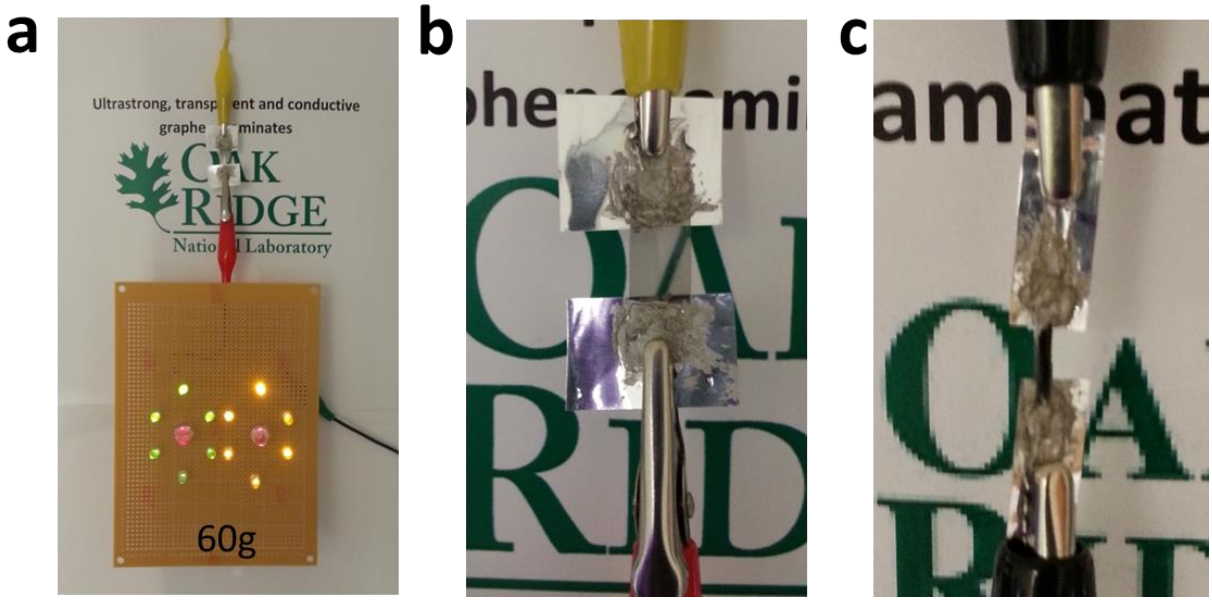

Figure S6. *LED (weighing 60 g) suspended on graphene laminates and graphene fibers.* Zoomed images demonstrate flexible transparent and electrically conductive graphene laminates (a,b) and fibers (c)

VII. Electrical conductivity measurements.

To measure electrical conductivity of the prepared laminates and fibers, samples were mounted either on a rigid substrate (SiO_2/Si wafer) or suspended between two pieces of aluminum foils (Fig 4 and FigS6). The resistance was measured in the 2-point scheme by a multimeter contacting silver epoxy on the sample's ends. Three different samples were prepared and measured.

$(Gr/PMMA)_{16}$. Resistivity, ρ, was calculated from the resistance (*R*), cross-section of the sample (*A*) and its length (*l*) using $\rho = R\frac{A}{l}$. For example, for the sample shown in Fig. 4a, the resistance was R ~ 150±15 Ω, length $l \sim (5\pm1)\cdot10^{-3}m$, and $A = 4.1\cdot10^{-6}m \cdot 0.01m$, where $w = 0.010\pm0.001m$ is the width of the sample and $4.1\cdot10^{-6}m$ –its thickness. It corresponds to $\rho \sim (1.2\pm0.3)\cdot10^{-3}\,\Omega\cdot$m and the electrical conductivity $1/\rho = 8.1\pm2.5$ S/cm. The contribution from graphene can be similarly estimated based on the $1.3\cdot10^{-3}$ of its volume fraction as $\rho \sim (1.6\pm0.4)\cdot10^{-6}\,\Omega\cdot$m and $1/\rho = (6.3\pm2)\cdot10^{3}$ S/cm

$(Gr)_6$. Fiber was mounted on SiO_2/Si wafer by silver epoxy. Resistivity was calculated in a similar way as for $(Gr/PMMA)_{16}$.From the measured parameters: $R \sim 100\pm15\,\Omega$, $l \sim (5\pm1)\cdot10^{-3}m$,

$A=n\cdot t\cdot w=6\cdot 0.33\cdot 10^{-9}m\cdot 0.05m$, $n=6$, $t=0.33\cdot 10^{-9}m$ and $w=0.050\pm 0.001m$, the resistivity was estimated: $\rho\sim(2.0\pm 0.4)\cdot 10^{-6}\Omega\cdot m$. Thus, the electrical conductivity of $(Gr)_6$ samples, $(5.0\pm 1.2)\cdot 10^3$ S/cm, is slightly less than the conductivity in laminates ($6.3\cdot 10^3$ S/cm) suggesting possible tears or ruptures in $(Gr)_6$ samples, as well as, different level of doping.

As a comparison, for the similarly transferred graphene onto SiO_2 substrate, the characteristic sheet resistance, ~1KΩ/sq, translates to resistivity $\rho \sim 3.3\cdot 10^{-7}\Omega\cdot m$ and the corresponding conductivity, $1/\rho \sim 3\cdot 10^4$ S/cm, is roughly 5-6 times higher than the measured here for laminates and fibers. It suggests that there may be imperfections in our procedure of sample preparation and further improvements could possibly lead to even better mechanical properties.

VIII. Modulus-Strength chart.

Figure S7 was compiled from various open sources: data for pure compounds were adapted from CES Edupack 2009 software [7]; carbon materials for composites: carbon fiber data - from Toray Industries product specifications[8], CNT ropes – from [9] and graphene oxide – from [10].

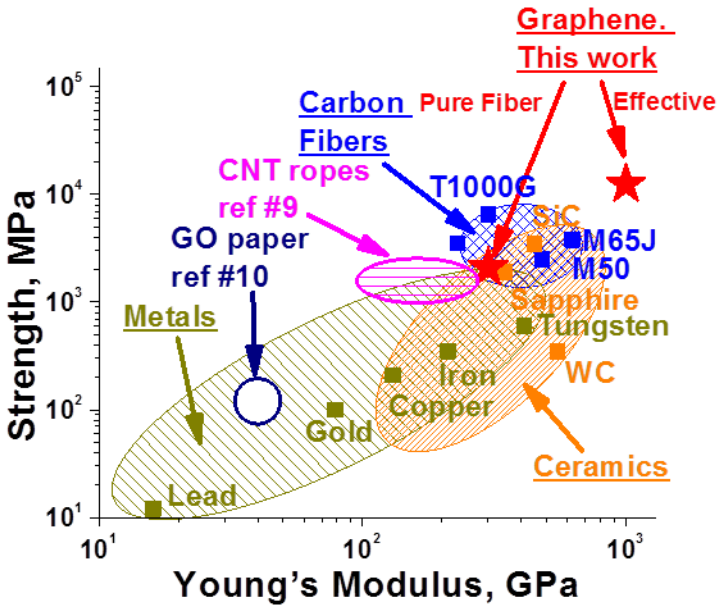

Figure S7. Strength-modulus chart for different materials. Results of this work are shown as red stars

IX. ***Calculation of the V_{PMMA} (volume fraction of PMMA), V_{Gr} (Volume fraction of Graphene), E_{Gr} (derived modulus of graphene) and σ_{Gr} (derived strength of graphene).***

Table S1 shows the experimental data along with the standard deviation calculated using at least three independent measurements: E_{PMMA} (modulus of 16 layer PMMA), σ_{PMMA} (strength of 16 layer PMMA), E_E and σ_E

Table S1. **Experimentally measured parameters**

Parameter	**Value**
E_{PMMA} (modulus of $(PMMA)_{16}$)	*2.5 ± 0.4 GPa*
σ_{PMMA} (strength of $(PMMA)_{16}$)	*53 ± 4 MPa*
E_E (modulus of $(PMMA/Gr)_{16}$)	*4 ± 0.5 GPa*
σ_E (strength of $(PMMA/Gr)_{16}$)	*67.1 ± 7.5 MPa*

Samples	*E, GPa*	*σ, MPa*	1/*ρ*, S/cm	E_{Gr}, *TPa*	σ_{Gr}, *GPa*	$1/\rho_{Gr}$, kS/cm
$(PMMA)_{16}$ laminate	2.5 ± 0.4	53 ± 4				
$(PMMA/Gr)_{16}$ laminate	4 ± 0.5	67.1 ± 7.5	8.1±2.5	1.2±0.5	11 ± 6.7	6.3 ± 2
$(PMMA)_1$ scroll		43.5± 15.5				
$(Gr)_1(PMMA)_1$ scroll		68 ± 7.7			19 ± 9	
$(Gr)_6(PMMA)_1$ scroll	4					
$(Gr)_6$ scroll	2.1		$(5.0±1.2)\cdot10^3$			5.0±1.2

In all calculations, the thickness of a monolayer graphene was taken to be equal to 0.33 nm. Our CVD samples are well characterized with continuous monolayer made of >10 μm grains and less than 5% of bilayer coverage (see refs.17,18 in main text). 16 layers of graphene have calculate thickness of 0.33nm*16=5.28nm~5.3nm.

To calculate the volumetric fraction of PMMA we used equation (S1):

$$V_{PMMA} = \frac{T_{PMMA}}{T_{PMMA}+5.3\ nm} = 1 - \frac{5.3\ nm}{T_{PMMA}+5.3\ nm} \qquad \text{(S1)}$$

where T_{PMMA} is the laminate thickness measured by profilometer (see Figure S3) and is primarily the thickness of PMMA. Thus the error for the volume fraction of PMMA (and graphene) we have used simple standard approach. [11] The error for V_{PMMA} is equal to:

$$\Delta_{V_{PMMA}} = \sqrt{\left(\frac{\partial V_{PMMA}}{\partial T_{PMMA}}\right)^2 \Delta^2_{T_{PMMA}}} = \left(\frac{\partial V_{PMMA}}{\partial T_{PMMA}}\right) \Delta_{T_{PMMA}} \quad \text{(S2)}$$

Where $\Delta_{V_{PMMA}}$ is the error for volume fraction of PMMA, $\Delta_{T_{PMMA}}$ is the error for film thickness (Figure S3). Using eq. S1 and S2 volume fractions of PMMA and graphene are equal to: $V_{PMMA}=0.9987\pm 2\cdot 10^{-4}$ and $V_{Gr}=(1.3\pm 0.2)\cdot 10^{-3}$

Similar approach was used to derive values for graphene modulus and strength.

Graphene modulus, E_{Gr} is calculated according to eq. S3 (rule of mixtures as shown in main text) and standard deviation according to S4.

$$E_{Gr} = \frac{E_E - E_{PMMA}\cdot(1-V_{Gr})}{V_{Gr}} \quad \text{(S3)}$$

$$\Delta_{E_{Gr}} = \sqrt{\left(\frac{\partial E_{Gr}}{\partial E_E}\right)^2 \Delta^2_{E_E} + \left(\frac{\partial E_{Gr}}{\partial E_{PMMA}}\right)^2 \Delta^2_{E_{PMMA}} + \left(\frac{\partial E_{Gr}}{\partial V_{Gr}}\right)^2 \Delta^2_{V_{Gr}}} \cong$$

$$\cong \frac{1}{V_{Gr}} \sqrt{\Delta^2_{E_E} + \Delta^2_{E_{PMMA}} + \left(\frac{E_E - E_{PMMA}}{V_{Gr}}\right)^2 \Delta^2_{V_{Gr}}} \quad \text{(S4)}$$

Where $\Delta_{E_E}, \Delta_{E_{PMMA}}, \Delta_{V_{Gr}}$ are standard deviations for $(Gr/PMMA)_{16}$ laminate (E_E), $(PMMA)_{16}$ laminate (E_{PMMA}) and volume fraction of graphene. Eqs. S3 and S4 yield $E_{Gr}=1.2\pm 0.5$ *TPa*. Analogous calculations for strength yield $\sigma_{Gr}=11\pm 6.7$ GPa

X. ***Estimation of the critical graphene volume fraction***

At low concentration of filler, the strength of the composite material may not follow the rule of mixtures and, instead, initially have a lower slope or even decrease upon adding filler, which can happen if the filler (graphene) fractures at a lower strain compared to the matrix (PMMA). The critical volume fraction, V'_{Gr}, at which the filler graphene will certainly increase the strength of the composite material can be estimated as:

$$V'_{Gr} = \frac{\sigma_{PMMA} - \sigma^*_{PMMA}}{\sigma_{Gr} + \sigma_{PMMA} - \sigma^*_{PMMA}} \quad \text{(S5)}$$

where σ_{PMMA} – strength of PMMA matrix, σ_{Gr} – graphene strength, and σ^*_{PMMA} - stress of the PMMA at a strain at which filler fracture occurs. [12]

Estimation of the lower bounds of V'_{Gr} by making $\sigma^*_{PMMA} = 0$ yields $V'_{Gr} = 5\cdot 10^{-3}$ which is approximately 4 times larger compared to our experimental volume fraction of graphene ($1.3\cdot 10^{-3}$), thus presented value $\sigma_{Gr}=11\pm 6.7$ GPa is rather on a lower bound.

XI. ***Details on Figure 4b***

In the references where only weight percentage of the filler was shown, we have recalculated the percentage to the volumetric using eq. S6.

$$\nu = \frac{w \cdot \rho_{polymer}}{w \cdot \rho_{polymer} + (1-w) \cdot \rho_{Gr}} \qquad \text{(S6)}$$

Where w is weight percentage, ν – volume percentage, $\rho_{polymer}$ – density of the polymer and ρ_{Gr} ~2.2 g/cm^3 – density of graphene

References.

1. Pandey, A.; Shyam, A.; Watkins, T.R.; Lara-Curzio, E.; Stafford, R.J.; Hemker, K.J. The Uniaxial Tensile Response of Porous and Microcracked Ceramic Materials, *J. Am. Ceram. Soc.* **2014**, *97*, 899-906
2. Donth E. The Glass Transition. Relaxation Dynamics in Liquids and Disordered Materials, *Springer*, Berlin, Germany, 2001
3. Bansal, A.;Yang, H.; Li, C.; Cho, K.; Benicewicz, B.C.; Kumar, S.K.; Schadler, L.S.; Quantitative Equivalence Between Polymer Nanocomposites and Thin Polymer Films, *Nat. Mat.* **2005**, *4*, 693-698
4. Alcoutlabi, M.; McKenna, G.B.; Effects of Confinement on Material Behavior at the Nanometre Size Scale, *J. Phys.: Condens. Matter.* **2005**, *17*, R461-R524
5. Tamai, Y.; Konishi, T.; Einaga, Y.; Fujii, M.; Yamakawa, H. Mean-Square Radius of Gyration of Oligo- and Poly(methyl methacrylate)s in Dilute Solutions, *Macromolecules* **1990**, *23*, 4067-4075
6. Jackson, C.; Chen, Y.-J.; Mays, J.W. Size Exclusion Chromatography with Multiple Detectors: Solution Properties of Linear Chains of Varying Flexibility in Tetrahydrofuran, *J. Appl. Polym. Sci.* **1996**, *61*, 865-874
7. Granta Design Edupack software website. http://www.grantadesign.com/education/edupack/index.htm (accessed Apr 27, 2015)
8. TORAYCA® Carbon fiber products. http://www.toraycfa.com/product.html (accessed Apr 27, 2015)
9. Lu, W.; Zu, M.; Byun, J.-H.; Kim, B.-S.; Chou, T.-W. State of the Art of Carbon Nanotube Fibers: Opportunities and Challenges. *Avd. Mater*. **2012**, *24*, 1805-1833
10. Dikin, D.A.; Stankovich, S.; Zimney, E.J.; Piner, R.D.; Dommett, G.H.B.; Evmenenko, G.; Nguyen, S.T.; Ruoff, R.S. Preparation and Characterization of Graphene Oxide Paper. *Nature* **2007**, *448*, 457-460
11. Ku H.H. Notes on the Use of Propagation of Error Formulas, *J. Res. Natl. Bur. Stand.* **1966,** 70C, 263-273
12. Kelly, A. and MacMillan, N.H. Strong Solids, Third Edition, Published in the United States by Oxford University Press, New York, USA, 1986